Inorganic Chemistry

ARTICLE

pubs.acs.org/IC

# Weak Ferromagnetism and Strong Spin−Spin Interaction Mediated by the Mixed-Valence Ethynyltetrathiafulvalene-Type Ligand

Junichi Nishijo, Ken Judai, and Nobuyuki Nishi*

Department of Materials Molecular Science, Institute for Molecular Science, 38 Nishigo-Naka, Myodaiji, Okazaki 444-8585, Japan

Supporting Information

**ABSTRACT:** A new chromium complex with ethynyltetrathiafulvalene (TTF)-type ligands, [CrCyclam(C≡C-5-methyl-4′5′-ethylenedithio-TTF)$_2$]OTf ([**1**]OTf), was synthesized. The cyclic voltammetry of the complex shows two reversible oxidation waves owing to the first and second oxidation of the TTF unit. The electrochemical oxidation of [**1**]OTf in a $Bu_4NClO_4$ or $Bu_4NBF_4$ solution of a 1:1 acetonitrile−chlorobenzene mixture gave isostructural crystals of [**1**][$ClO_4$]$_2$(PhCl)$_2$(MeCN) and [**1**][$BF_4$]$_2$(PhCl)$_2$(MeCN), where two mixed-valence TTF units of adjacent complexes form a dimer radical cation. The crystal structures are characterized by an alternating chain of $S = {}^3/_2$ $Cr^{3+}$Cyclam units and $S = {}^1/_2$ $(TTF)_2^+$ dimers. These two paramagnetic components are connected directly by an ethynyl group, resulting in a strong intrachain spin−spin interaction of $2J/k_B = -30$ and $-28$ K for $[ClO_4]^-$ and $[BF_4]^-$ salts, respectively ($H = -2J\Sigma_i S_i \cdot S_{i+1}$). Both salts show a weak ferromagnetic transition at 23 K thanks to interchain antiferromagnetic interaction between TTF dimers. The remanent magnetizations and coercive forces of nonoriented samples at 1.8 K are 0.016 $\mu_B$ and 90 mT for the $[ClO_4]^-$ salt and 0.010 $\mu_B$ and 50 mT Oe for the $[BF_4]^-$ salt, respectively. The weak ferromagnetism is attributed to the Dzyaloshinsky−Moriya interaction between adjacent TTF dimers and/or the single-ion anisotropy of $[\mathbf{1}]^{2+}$.

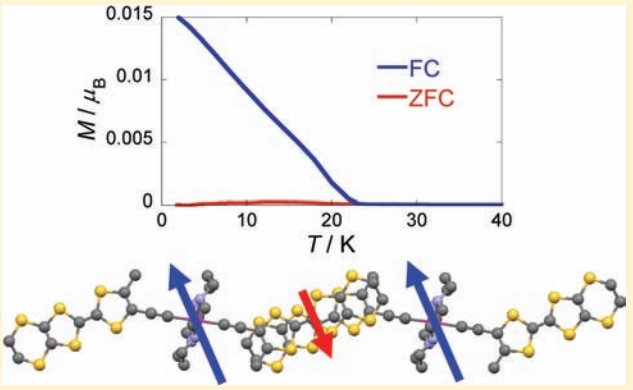


## INTRODUCTION

In recent years, hybrid "π−d interaction systems" have been intensively investigated in the research fields of organic conductors and molecule-based magnets,[1] where the interaction between π and d electrons brings various interesting phenomena such as large negative magnetoresistance,[2] magnetically suppressed superconductivity,[3] and field-induced superconductivity.[4] These cooperative features of the π−d interaction systems are promising to achieve multifunctional molecule-based devices. In almost all cases, however, π−d interactions are regrettably not as strong in the present stage because the localized magnetic electrons and the conducting electrons are separately placed on different molecules. One of the effective strategies to overcome this shortcoming is the direct coordination of tetrathiafulvalene (TTF)-type conductive molecules to paramagnetic transition-metal cations through intervening functional groups.[5] Direct coordination unifies π- and d-electron systems into a single molecule, and it is expected that the interaction between the two systems becomes extremely stronger than that in conventional separated π−d systems. In addition, such "directly coordinated" complexes are also interesting in the context of the molecule-based magnetic materials. Because of the planar molecular shape and the vertically oriented π orbital of the TTF backbone, the strength of the spin−spin exchange interaction $2|J|/k_B$ between TTF radicals can become stronger than 300 K,[6] where $k_B$ is the Boltzmann constant and $J$ is defined in the following Hamiltonian:

$$H = -2J\sum_i S_i S_{i+1} \quad (1)$$

The strong intermolecular exchange interaction leads to a higher transition temperature in cooperation with a strong intramolecular exchange interaction.

In the present paper, we report on the synthesis, crystal structures, and magnetic properties of a new chromium complex with TTF-based ligands. Among the several candidates, we employed an ethynyl group and a chromium atom as a coordination functionality and a magnetic metal cation, respectively. The ethynyl group is known as a suitable functional group for connecting two electronic systems.[5h,i,7] Especially, the high stability of chromium acetylide complexes is appropriate for the construction of a molecule-based magnet.[8] The obtained new chromium acetylide−TTF-type complex [CrCyclam(C≡C-5-methyl-4′5′-ethylenedithio-TTF)$_2$]$^+$ ([**1**]$^+$; Cyclam = 1,4,8,11-tetraazacyclotetradecane) is a redox-active complex, and its oxidation state shows a strong spin−spin exchange interaction.

**Received:** November 30, 2010
**Published:** March 11, 2011

**Scheme 1. Synthesis Route of [1]OTf[a]**

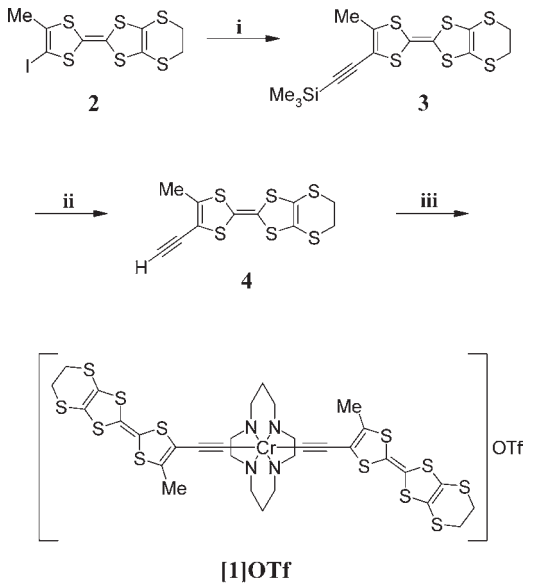


[a] Reagents and conditions: (i) (trimethylsilyl)acetylene, $Pd(Ph_3P)_4$, CuI, THF; (ii) KF, THF−methanol; (iii) lithium diisopropylamide, [CrCyclam$(OTf)_2$]OTf, THF, −78 °C.

## EXPERIMENTAL SECTION

**Preparation of the Compounds.** The precursors 4-iodo-5-methyl-4′,5′-ethylenedithiotetrathiafulvalene (**2**) and [CrCyclam$(OTf)_2$]-OTf (OTf = trifluoromethanesulfonate) were prepared according to the literature.[9] The synthesis route of [**1**]OTf is illustrated in Scheme 1. Single crystals of dication salts [**1**][$ClO_4$]$_2$(PhCl)$_2$(MeCN) and [**1**][$BF_4$]$_2$(PhCl)$_2$(MeCN) were obtained by the galvanostatic oxidation of [**1**]OTf (14 mg) in 20 mL of a $Bu_4NClO_4$ or $Bu_4NBF_4$ (30 mg) solution of a 1:1 chlorobenzene−acetonitrile mixture (0.6 $\mu$A, 2−3 weeks). [**1**][$ClO_4$]$_2$(PhCl)$_2$(MeCN) was obtained as black rod-shaped crystals, while [**1**][$BF_4$]$_2$(PhCl)$_2$(MeCN) was obtained as small black blocks. IR (KBr): 2065 cm$^{-1}$ ($\nu_{C\equiv C}$) for both [$ClO_4$]$^-$ and [$BF_4$]$^-$ salts.

**4-[(Trimethylsilyl)ethynyl]-5-methyl-4′5′-ethylenedithio-tetrathiafulvalene (3).** Under an argon atmosphere, 2.25 g (5.16 mmol) of **2**, 0.72 mL (5.2 mmol) of (trimethylsilyl)acetylene, 1 g (0.86 mmol) of $Pd(Ph_3P)_4$, 248 mg (1.3 mmol) of CuI, and 2 mL of *N*,*N*′-diisopropylamine were added to 200 mL of degassed, dehydrated tetrahydrofuran (THF). After 48 h of stirring at room temperature, the solution was concentrated in vacuo. The residual was dissolved in 300 mL of dichloromethane. Insoluble impurities were removed by filtration, and then the solution was concentrated again. The crude product was purified by silica gel chromatography using 1:1 dichloromethane−hexane as the eluent. **3** was obtained as an orange powder (yield: 1.47 g, 70%). Mp: 178 °C. IR (KBr): 2138 cm$^{-1}$ ($\nu_{C\equiv C}$). $^1$H NMR ($\delta$, $CDCl_3$, 400 MHz): 3.28 (s, 4H, $C_2H_4$), 2.13 (s, 3H, $CH_3$), 0.21 (s, 9H, Si($CH_3$)$_3$). $^{13}$C NMR ($\delta$, $CDCl_3$, 100 MHz): 138.87 (C), 115.14 (C), 114.28 (C), 113.90 (C), 110.16 (C), 106.39 (C), 102.38 (C), 94.83 (C), 30.40 ($C_2H_4$), 15.99 ($CH_3$), 0.00 [Si($CH_3$)$_3$]. Anal. Calcd for $C_{14}H_{16}S_6Si$: C, 41.54; H, 3.98; S, 47.53. Found: C, 41.43; H, 4.11; S, 47.68.

**4-Ethynyl-5-methyl-4′5′-ethylenedithiotetrathiafulvalene (4).** Under an argon atmosphere, 810 mg (2 mmol) of **3** and 580 mg (10 mmol) of KF were added to 50 mL of a 1:1 THF−methanol mixed solution. After 24 h of stirring at room temperature, 200 mL of water was added and extracted with 300 mL of dichloromethane. The organic layer was concentrated and purified by silica gel chromatography using dichloromethane as the eluent. **3** was obtained as a reddish-orange powder (yield: 595 mg, 90%). Mp: 133−138 (dec). IR (KBr): 2094 cm$^{-1}$ ($\nu_{C\equiv C}$). $^1$H NMR ($\delta$, $CDCl_3$, 400 MHz): 3.35 (s, 1H, ≡C*H*), 3.29 (s, 4H, $C_2H_4$), 2.16 (s, 3H, $CH_3$). $^{13}$C NMR ($\delta$, $CDCl_3$, 100 MHz): 139.55 (C), 115.14 (C), 114.67 (C), 114.08 (C), 113.73 (C), 84.00 (≡CH), 74.42 (C), 30.17 ($C_2H_4$), 15.67 ($CH_3$). Anal. Calcd for $C_{11}H_8S_6$: C, 39.73; H, 2.42; S, 57.85. Found: C, 39.80; H, 2.23; S, 58.01.

**[CrCyclam(C≡C-5-methyl-4′5′-ethylenedithio-TTF)$_2$]OTf ([1]OTf).** Under an argon atmosphere, 1.33 g (4 mmol) of **4** was dissolved in 35 mL of dehydrated THF. The solution was cooled to −78 °C, and then 3.8 mmol of a lithium diisopropylamide solution was slowly added. After 3 h of stirring at −78 °C, 1 g (1.43 mmol) of [CrCyclam$(OTf)_2$](OTf) was added, and the solution was stirred for 3 h again. The solution was slowly warmed to room temperature, and ca. 1 mL of water, followed by 200 mL of dichloromethane, was added. The solution was dried by $MgSO_4$ and filtered. The filtrate was concentrated and purified by silica gel chromatography using a 7:3 dichloromethane−acetonitrile mixture as the eluent. The obtained solution was concentrated and diluted with ca. 300 mL of diethyl ether. [**1**]OTf was obtained as an orange powder (yield: 840 mg, 55%). IR (KBr): 2058 cm$^{-1}$ ($\nu_{C\equiv C}$). Anal. Calcd for $C_{33}H_{38}CrF_3N_4O_3S_{13}$: C, 37.23; H, 3.60; N, 5.26; S, 39.16. Found: C, 37.13; H, 3.60; N, 5.15; S, 39.24.

**Table 1. Crystal Data and Structure Refinement for [1][$ClO_4$]$_2$(PhCl)$_2$(MeCN) and [1][$BF_4$]$_2$(PhCl)$_2$(MeCN)**

| | [1][$ClO_4$]$_2$(PhCl)$_2$(MeCN) | [1][$BF_4$]$_2$(PhCl)$_2$(MeCN) |
|---|---|---|
| mol formula | $C_{46}H_{51}Cl_4CrN_5O_8S_{12}$ | $C_{46}H_{51}B_2Cl_2CrF_8N_5S_{12}$ |
| fw | 1380.44 | 1355.16 |
| temp/K | 293(2) | 293(2) |
| radiation, $\lambda$/Å | 0.710 3 | 0.710 3 |
| cryst syst | monoclinic | monoclinic |
| space group | *C*2/*c* (No. 15) | *C*2/*c* (No. 15) |
| *a*/Å | 32.921(4) | 32.828(3) |
| *b*/Å | 11.8484(11) | 11.8716(11) |
| *c*/Å | 16.1400(16) | 16.1111(16) |
| α/deg | 90 | 90 |
| $\beta$/deg | 103.151(3) | 103.469(3) |
| $\gamma$/deg | 90 | 90 |
| *V*/Å$^3$ | 6130.4(11) | 6106.1(10) |
| *Z* | 4 | 4 |
| $d_{calc}$/g cm$^{-3}$ | 1.496 | 1.474 |
| unique reflns | 7593 | 7850 |
| $I > 2\sigma I$ | 5697 | 6150 |
| final R1,[a] wR2[b] | 0.0946, 0.2882 | 0.0901, 0.2844 |

[a] $R = \Sigma||F_o| - |F_c||/\Sigma|F_o|$. [b] $wR2 = \{\Sigma[w(F_o^2 - F_c^2)^2]/\Sigma[w(F_o^2)^2]\}^{1/2}$.

**Single-Crystal Structure Determinations.** X-ray diffraction measurements were carried out on a Rigaku AFC-7R four-circle diffractometer (fine-focus type) with a Mercury CCD area detector at 293 K, using Mo Kα radiation ($\lambda$ = 0.7107 Å). The structures were solved using direct methods (*SIR2004*)[10] and then refined with a full-matrix least-squares method (*SHELXL-97*).[11] A numerical absorption correction was introduced. All non-hydrogen atoms except the disordered acetonitrile molecule were refined anisotropically. Hydrogen atoms were placed in their calculated positions and refined by the riding model. Crystallographic data are summarized in Table 1. Full bond lengths and angles, atomic coordinates, and complete crystal structure results are deposited as Supporting Information.

**Physical Measurements.** Cyclic voltammetry (CV) experiments were carried out at a scan rate of 100 mV s$^{-1}$ in a 0.1 M acetonitrile


dx.doi.org/10.1021/ic102384s |*Inorg. Chem.* 2011, 50, 3464–3470

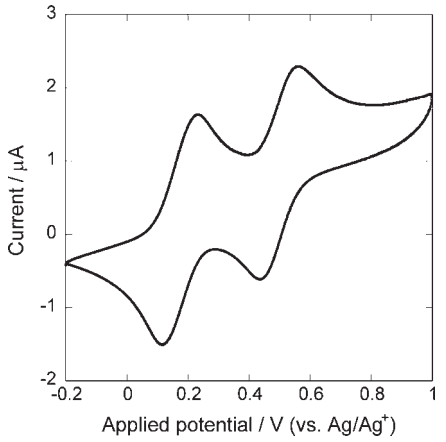


**Figure 1.** CV measurement of [**1**]OTf in a 0.1 M acetonitrile solution of $Bu_4NClO_4$.

solution of $Bu_4NClO_4$ by using a potentiostat (Hokuto Denko, HSV-100), platinum working and counter electrodes, and a $Ag/Ag^+$ (0.01 M $AgNO_3$, 0.3 V vs SCE) reference electrode. Direct-current magnetic susceptibilities were measured by using a Quantum-Design MPMS-XL7 SQUID magnetometer for randomly oriented single crystals encapsulated in aluminum capsules in a temperature range of 1.8−300 K. The paramagnetic contribution of the capsules was calculated based on the weight of the capsules and the standard temperature-dependent susceptibility of the capsules. Diamagnetic corrections were estimated from Pascal's constants as $-496 \times 10^{-6}$, $-678 \times 10^{-6}$, and $-688 \times 10^{-6}$ emu $mol^{-1}$ for [**1**]OTf, [**1**][$ClO_4$]$_2$(PhCl)$_2$(MeCN), and [**1**][$BF_4$]$_2$-(PhCl)$_2$(MeCN), respectively. Anisotropic magnetization was also measured for an assembly of aligned single crystals of the $[ClO_4]^-$ salt thanks to its large crystal size, where the *c* axis, the longest axis of the crystals, could be distinguished from the other two axes, while the *a* and *b* axes are indistinguishable. The electron spin resonance (ESR) spectra for nonoriented microcrystalline samples were measured with a Bruker E-500 (X band, continuous wave) spectrometer.

## RESULTS AND DISCUSSION

**Synthesis and Electrochemical Properties.** The synthetic route of molecule **4** shown in Scheme 1 is basically the same as that of ethynyltrimethyltetrathiafulvalene[5i] except using a THF−methanol mixture in the elimination process of the trimethylsilyl group because of the lower solubility of molecule **3**. The preparation method of [**1**]OTf was slightly modified from that of [CrCyclam(C≡CPh)$_2$]OTf.[9d] Lithium diisopropylamide was used as a substitute for butyllithium, and [CrCyclam(OTf)$_2$]OTf was added at a temperature of −78 °C. These two modifications are indispensable in avoiding decomposition of ligand **4**. The stretching frequency of the C≡C triple bond is found at 2138, 2094, and 2058 $cm^{-1}$ for **3**, **4**, and [**1**]OTf, respectively. The difference between these three frequencies is quite similar to those of 1-phenyl-2-(trimethylsilyl)acetylene (2159 $cm^{-1}$), phenylacetylene (2110 $cm^{-1}$), and [CrCyclam(C≡CPh)$_2$]OTf (2077 $cm^{-1}$), suggesting that the electronic structure of the coordination bond of $[\mathbf{1}]^+$ is roughly the same as that of the stable complex $[CrCyclam(C{\equiv}CPh)_2]^+$.

The result of the CV measurement of [**1**]OTf in acetonitrile is shown in Figure 1. The complex shows two reversible oxidation waves at 0.174 and 0.498 V (vs $Ag/Ag^+$). The values of the redox potentials are very similar to the values reported for 4, 5-dimethyl-4′,5′-ethylenedithiotetrathiafulvalene (0.15 and 0.49 V vs $Ag/Ag^+$);[12] therefore, these reversible oxidations are attributed to the first and second oxidation of the coordinated TTF units. The presence of only two oxidation peaks indicates that the Coulombic interaction between the two TTF units in a complex is weak, as is frequently observed in the case of the complex containing two TTF-based ligands.[5c,d]

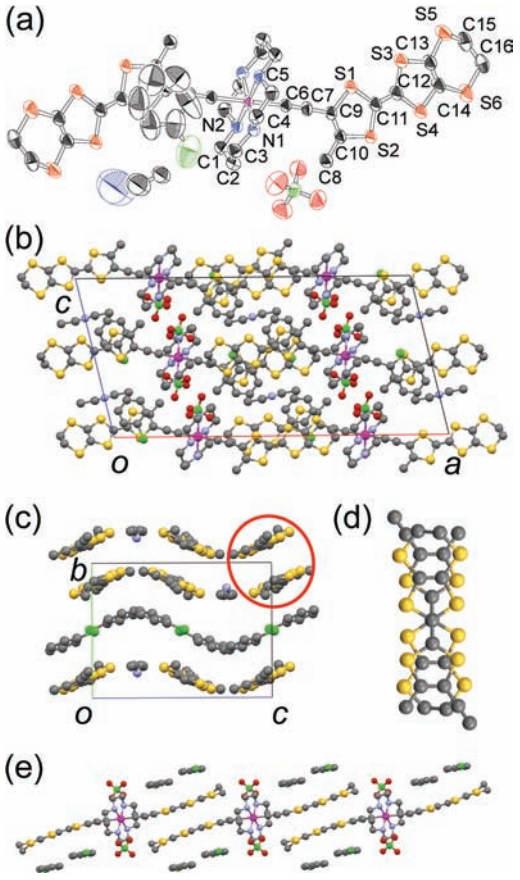


**Figure 2.** (a) ORTEP[13] drawing (50% probability) of the molecular structure with the atomic numbering scheme of [**1**][$ClO_4$]$_2$(PhCl)$_2$(MeCN). Hydrogen atoms are omitted for clarity. (b) Crystal structure of [**1**][$ClO_4$]$_2$(PhCl)$_2$(MeCN) viewed along the *b* axis. (c) Structure of a ligand layer viewed along the *a* axis. The red circle indicates a dimer structure of ligands. (d) Stacking manner of a ligand dimer. (e) 1D chain structure of $[\mathbf{1}]^{2+}$ complexes elongated parallel to the $a + b$ axis.

**Crystal Structures.** The crystal structure of [**1**][$ClO_4$]$_2$-(PhCl)$_2$(MeCN) is shown in Figure 2. Because the crystal structure of the $[BF_4]^-$ salt is the same as that of the $[ClO_4]^-$ salt except the anion, we discuss only the structure of the $[ClO_4]^-$ salt in the following. The asymmetric unit of the crystal consists of a half cation, one anion, and solvents with disorder of an acetonitrile molecule. The cation-to-anion ratio of 1:2 indicates a divalent state of complex $[\mathbf{1}]^{2+}$. Judging from the result of the CV measurement, the additional positive charge is attributed to oxidation of the TTF units, which is also evidenced by the planar structure of the TTF backbones. The bond length of 1.211(5) Å between C6 and C7 is a typical value of the C≡C triple bond and is not affected by oxidation. The crystal structure of the salt is characterized by two kinds of layers stacked alternately along the *a* axis. The first layer consists of $Cr^{3+}$Cyclam units and $[ClO_4]^-$ anions, while the second layer consists of oxidized ligands, chlorobenzene, and acetonitrile molecules. In


dx.doi.org/10.1021/ic102384s |*Inorg. Chem.* 2011, 50, 3464–3470

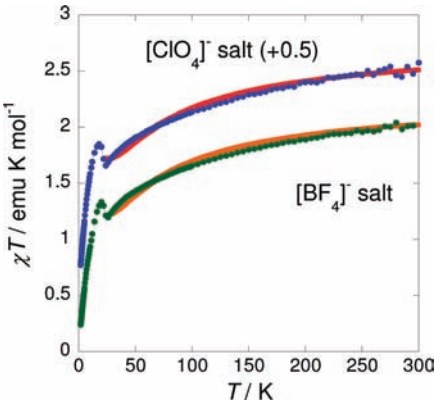


**Figure 3.** Temperature dependences of the $\chi T$ values for the nonoriented samples of the $[ClO_4]^-$ (blue) and $[BF_4]^-$ (green) salts, where the data for the $[ClO_4]^-$ salt are vertically shifted up by 0.5 for clarity. The red and orange solid lines are the fitted curves by using eq 2 with the fitting parameters of $2J/k_B = -30$ K and $2zJ'/k_B = -2$ K for the $[ClO_4]^-$ salt (also vertically shifted) and $2J/k_B = -28$ K and $2J'/k_B = -1.9$ K for the $[BF_4]^-$ salt (see the text).

the first layer, each $Cr^{3+}$Cyclam unit is separated by adjacent anions. In the second layer, the two neighboring TTF backbones form a dimer unit, where one dimer unit has one cationic charge. The intradimer stacking manner of the TTF units shown in Figure 2d is quite similar to that of $\kappa$-type organic conductors.[3] This stacking manner and the short intradimer distance of 3.377(8) Å for C12−C12 suggest that one cationic charge of the dimer is delocalized over the dimer. In other words, the TTF unit is in a mixed-valence state. There is only one short interdimer contact (S2−S6) between two adjacent dimers, where the interatomic distance of 3.854(2) Å is slightly longer than the sum of the van der Waals radii (1.85 Å for the sulfur atom). This contact weakly binds the dimers in the $c$ direction, while the dimers are completely separated by chlorobenzene molecules in the $b$ direction, as shown in Figure 2c. The mixed-valence $(TTF)_2^+$ dimers and $Cr^{3+}$Cyclam units are connected by the ethynyl groups and form one-dimensional (1D) chains, like in the case of $[Cu(hfac)2(TTF\text{-}py)_2](PF_6)(C_2H_2Cl_2)_2$,[5j] along the $a + b$ and $a - b$ axes.

**Magnetic Properties.** The molar magnetic susceptibility $\chi$ of [**1**]OTf obeys the Curie−Weiss law with a Curie constant of 1.89 emu K $mol^{-1}$ and a negligibly small Weiss temperature of −0.1 K. No magnetic transition was observed down to 1.8 K. The observed Curie constant is in good agreement with the spin-only value of $S = {}^3/_2$ $Cr^{3+}$ (1.875) and consistent with the neutral state of the ligands expected from the CV measurement.

The temperature dependences of the $\chi T$ values for the $[ClO_4]^-$ and $[BF_4]^-$ salts measured under an external field of 0.1 T are almost identical, as shown in Figure 3. The observed $\chi T$ values at 300 K, 2.07 and 2.04 emu K $mol^{-1}$ for the $[ClO_4]^-$ and $[BF_4]^-$ salts, respectively, are slightly smaller than the summation value of free $S = {}^1/_2$ (0.375) and $S = {}^3/_2$ (1.875) spins owing to the antiferromagnetic interaction. As discussed later, the interaction is strong and cannot be ignored even at room temperature. Therefore, it is not surprising that the observed $\chi T$ values at room temperature are smaller than those expected for the free spins. Indeed, the observed values are in good agreement with the theoretical values of 2.01 emu K $mol^{-1}$ for the $[ClO_4]^-$ salt and 2.03 emu K $mol^{-1}$ for the $[BF_4]^-$ salt,

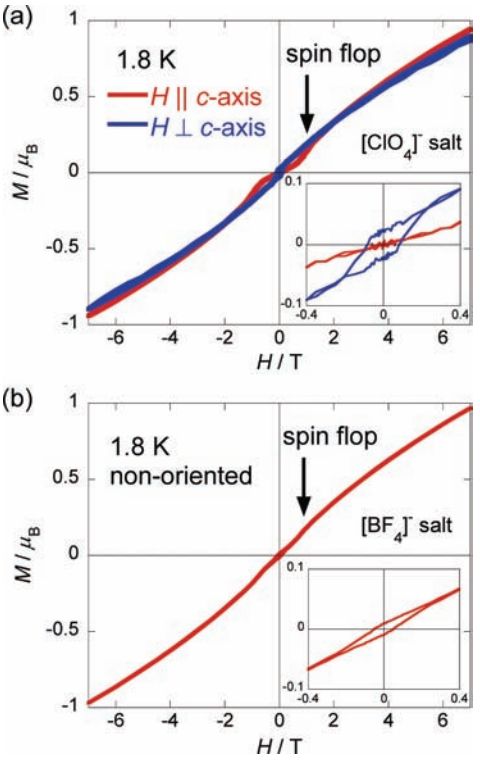


**Figure 4.** Magnetization curves of the (a) aligned $[ClO_4]^-$ and (b) nonoriented $[BF_4]^-$ crystals. The insets are the enlarged parts at low field.

calculated by using eq 2 and the obtained fitting parameters discussed later. The $\chi T$ values gradually decrease as the temperature decreases and take a minimum of 1.16 and 1.20 emu K $mol^{-1}$ at 24 K for the $[ClO_4]^-$ and $[BF_4]^-$ salts, respectively. Below the temperature, the values show a small jump at around 23 K, followed by a rapid decrease due to the magnetic transition discussed later. Judging from the 1D alternating chain structure of $S = {}^3/_2$ $Cr^{3+}$Cyclam units and $S = {}^1/_2$ $(TTF)_2^+$ dimers, it is plausible that the spin structure of the salts is approximately 1D ferrimagnetic with strong intrachain and weaker interchain interactions. To estimate the strength of the intrachain interaction, the following analytical expression for the $\chi T$ value of weakly interacting $[{}^1/_2 - {}^3/_2]$ ferrimagnetic chains[8,14] is used, where the interchain interaction is treated in the mean-field approximation.

$$\chi T = \chi_{1D} T \left(1 + \frac{\alpha \chi_{1D}}{1 - \alpha \chi_{1D}}\right) \tag{2}$$

$$\chi_{1D} = \frac{1}{T}\left\{0.5756\left(\frac{|2J|}{k_B T}\right)^{1.80} + 2.250 \exp\left(-0.882\frac{|2J|}{k_B T}\right)\right\} \tag{3}$$

$$\alpha = \frac{2zJ'}{g^2 \mu_B{}^2 N} \tag{4}$$

where $\chi_{1D}$, $k_B$, $g$, $\mu_B$, $N$, $J$ and, $zJ'$ are the susceptibility of the isolated $[{}^1/_2 - {}^3/_2]$ ferrimagnetic chain, the Boltzmann constant, the $g$ value ($g = 2$ is used for simplicity), the Bohr magneton, the Avogadro constant, the intrachain exchange interaction defined


dx.doi.org/10.1021/ic102384s |Inorg. Chem. 2011, 50, 3464–3470

in eq 1, and the fitting parameter representing the number and strength of the effective interchain interaction in the mean-field approximation, respectively. The best fit of the $\chi T$ values in the temperature range from 23 to 300 K gives the values of the intrachain interaction $2J/k_B = -30$ and $-28$ K for the $[ClO_4]^-$ and $[BF_4]^-$ salt, and the effective interchain interaction $2zJ'/k_B = -2$ and $-1.9$ K for the $[ClO_4]^-$ and $[BF_4]^-$ salt, respectively, where the small difference of the values between the salts is probably not significant. The considerably strong intrachain interaction is a natural consequence of the direct coordination of the TTF-type ligand. In the crystal, intrachain interaction also means the intramolecular interaction between the $Cr^{3+}$ cation and a mixed-valence TTF-type radical, where the two magnetic components are directly connected through the $\pi$ orbital of the coordinating ethynyl group. The weak interchain interaction is mediated by the interdimer contact between S2 and S6 atoms. The weakness of the interchain interaction is due to the long distance of the contact, as mentioned previously.

Figure 4 shows the magnetization curves of an assembly of aligned (but random in the plane perpendicular to the $c$ axis) and nonoriented single crystals of the $[ClO_4]^-$ and $[BF_4]^-$ salts, respectively, at 1.8 K. When the field is applied perpendicular to the $c$ axis, the $[ClO_4]^-$ salt shows a small hysteresis loop with a remanent magnetization of 0.021 $\mu_B$ and a coercive force of 90 mT, suggesting the weak ferromagnetic ground state. In contrast to the case of $H$ perpendicular to the $c$ axis, no spontaneous magnetization is observed with the applied field parallel to the $c$ axis, while the rapid increase of magnetization occurs at around $H = 1$ T thanks to the spin-flop transition. In the case of nonoriented crystals of the $[ClO_4]^-$ salt, the observed values of remanent magnetization, coercive force, and spin-flop field are 0.016 $\mu_B$, 90 mT, and 1 T, respectively. The existence of the spin-flop transition and the absence of remanent magnetization in the case of $H$ parallel to the $c$ axis indicate that the spin-easy axis of the $[ClO_4]^-$ salt is parallel to the $c$ axis. In addition, the orthogonality of the spin-easy axis ($c$ axis) and the spontaneous magnetization direction (parallel to the $c$ axis) clearly evidence the canted weak ferromagnetism. Although the observed remanent magnetization is an average value of randomly oriented crystals, we can estimate the actual value of the remanent magnetization by using the following arithmetic average of the direction cosine of the two- or three-dimensional (2D or 3D) randomly oriented unit vector.

$$\text{average value (2D)} = \frac{1}{\pi}\int_{-\pi/2}^{\pi/2} \cos\theta \, d\theta = \frac{2}{\pi} \qquad (5)$$

$$\text{average value (3D)} = \frac{1}{2\pi}\int_{0}^{\pi/2} 2\pi \sin\theta \cos\theta \, d\theta = \frac{1}{2} \qquad (6)$$

The calculated actual remanent magnetization of the $[ClO_4]^-$ salt is 0.033 $\mu_B$ based on eq 5 and a value of 0.021 $\mu_B$ for oriented crystals and 0.032 $\mu_B$ based on the eq 6 and a value of 0.016 $\mu_B$ for nonoriented crystals. Therefore, the spin-canting angle of $[^1/_2 - {}^3/_2]$ ferrimagnetic chains is calculated as $\sin^{-1}[0.033\,\mu_B/(3\,\mu_B - 1\,\mu_B)] = 0.95°$. The weak ferromagnetic behavior is also observed in the nonoriented $[BF_4]^-$ salt, but a coercive force of 50 mT and a remanent magnetization of 0.010 $\mu_B$ are significantly smaller than those of the nonoriented $[ClO_4]^-$ salt. The actual remanent magnetization is also calculated as 0.020 $\mu_B$, which corresponds to a canting angle of 0.57°. The different canting angles and coercive forces of the two salts are probably caused by the small structural disparity between the salts, but the detailed mechanism remains unclear. The spin-flop field of 0.9 T in the $[BF_4]^-$ salt is also smaller than that of the $[ClO_4]^-$ salt, but the difference is not as large.

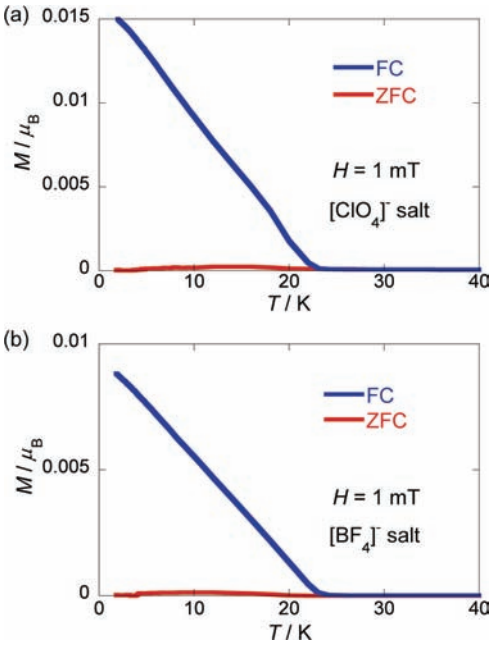


**Figure 5.** FC (1 mT) and ZFC magnetizations of the nonoriented (a) $[ClO_4]^-$ and (b) $[BF_4]^-$ salts measured at 1 mT.

The field-cooled (FC) and zero-field-cooled (ZFC) magnetizations of the nonoriented crystals are shown in Figure 5. The temperature dependences of the magnetizations of two salts are very similar to each other, except their magnitudes. The FC magnetization linearly decreases as the temperature increases, while the ZFC magnetization remains approximately zero. The FC magnetization of both salts coincides with the ZFC magnetizations just above 23 K, implying that a weak ferromagnetic transition occurs at that temperature.

**ESR Measurements.** The ESR spectrum of the monovalent salt [**1**]OTf gives two Gaussian peaks at the $g$ values of 3.07 and 1.54 with broad peak-to-peak line widths ($\Delta H_{pp}$) of 82 and 70 mT, respectively, and these values are close to the case of $[CrCyclamCl_2]Cl$.[15] The Gaussian line shape indicates that the exchange interaction between $Cr^{3+}$ ions is very weak and is congruous with the magnetic susceptibility of [**1**]OTf, where only a negligibly small exchange interaction was observed, as mentioned previously.

The spectra of the divalent salts of the $[ClO_4]^-$ and $[BF_4]^-$ anions are approximately identical and are characterized by a single Lorentzian in the whole temperature range without separation of the spins on the $Cr^{3+}$ cations and TTF radical dimer units, suggesting the existence of an exchange interaction between these two spin systems. The temperature dependences of the $g$ and $\Delta H_{pp}$ values of the salts are shown in Figure 6. The $g$ values, 1.991 for both salts, at room temperature are quite close to the value of six-coordinated $Cr^{3+}$ systems,[15,16] suggesting that the signal mainly comes from the $Cr^{3+}$ spins. The observed line widths $\Delta H_{pp} = 6.6$ and 7.2 mT for the $[ClO_4]^-$ and $[BF_4]^-$ salts at room temperature are obviously smaller than not only the value of the monovalent salt (>70 mT) but also the dipolar width


dx.doi.org/10.1021/ic102384s |Inorg. Chem. 2011, 50, 3464–3470

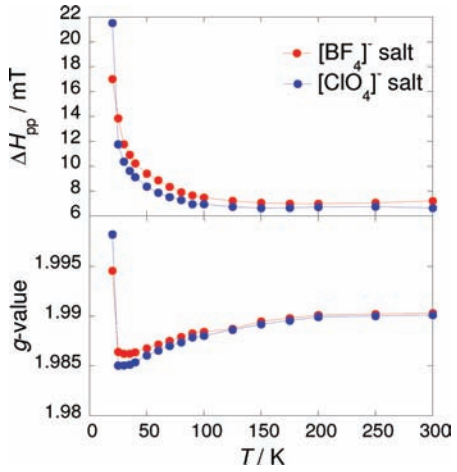


**Figure 6.** Temperature dependences of the ESR peak-to-peak line widths ($\Delta H_{pp}$, top) and $g$ values (bottom) for the $[ClO_4]^-$ and $[BF_4]^-$ salts.

of 17.5 mT (calculated based on the crystal structure and averaged for all directions), showing the effect of exchange narrowing. The line widths remain unchanged above 150 K. Below that temperature, $\Delta H_{pp}$ increases as the temperature decreases and diverges at around a weak ferromagnetic transition temperature of 23 K. The $g$ values show plateau behavior above 175 K. Below that temperature, the values gradually decrease with a decrease in the temperature to minimum values of 1.985 and 1.986 for the $[ClO_4]^-$ and $[BF_4]^-$ salts at around 30 K, followed by sharp increases corresponding to the weak ferromagnetic transition. The moderate increase of $\Delta H_{pp}$ and decrease of the $g$ value are the signature of the short-range order of the spin systems and are often observed in low-dimensional magnetic materials.[2c,17] The existence of short-range order is consistent with the 1D ferrimagnetic structure of the $[ClO_4]^-$ and $[BF_4]^-$ salts.

**Origin of Weak Ferromagnetism.** At the end of this section, we briefly discuss the origin of weak ferromagnetism. There is no doubt that the spin structure of $[\mathbf{1}][anion]_2(PhCl)_2(MeCN)$ is characterized by the ferrimagnetic chain of $Cr^{3+}$ ($S = {}^3/_2$) and the $(TTF)_2^+$ dimer ($S = {}^1/_2$) evidenced by both the crystal structure and the good agreement between the numerical fittings and the experimental results of the $\chi T$ value. Therefore, the weak ferromagnetism is caused by the noncollinear spin alignment of the ferrimagnetic chains. The first candidate for the noncollinear spin structure is the single-ion anisotropy of $[\mathbf{1}]^{2+}$. The uniaxial $C-CrN_4-C$ coordination structure of $[\mathbf{1}]^{2+}$ has $D_{4h}$ symmetry, which leads to the single-ion anisotropy of the complex. In addition, hybridization between the d orbital of $Cr^{3+}$ and the $\pi$ orbital of the TTF radical can also cause anisotropy. Because the two adjacent complexes in neighboring ferrimagnetic chains are related by not an inversion symmetry but a 2-fold axis, the effect of the single-ion anisotropy is not canceled out and can bring a canted spin structure. The second candidate for the noncollinear spin structure is the Dzyaloshinsky–Moriya (DM) interaction.[18] As mentioned previously, the interchain interaction is caused by the interaction between the ligand dimers. The adjacent dimers are, like in the adjacent complexes, related by a 2-fold axis, and there is no inversion center between the adjacent dimers. The absence of an inversion center can bring the DM interaction, which prefers canted spin arrangements. Therefore, the origin of the weak ferromagnetism can be ascribed to canting of the magnetic anisotropy axes of adjacent complexes and/or the DM interaction between the adjacent ligand dimers.

## CONCLUSION

The synthesis, electrochemical properties, crystal structures, and magnetic properties of the first chromium acetylide–TTF-type complex $[\mathbf{1}]^+$ and its radical cation salts are reported. The complex shows two reversible redox peaks due to the oxidation state of TTF-type ligands. The electrochemical oxidation of $[\mathbf{1}]^+$ in a solution of the $[ClO_4]^-$ or $[BF_4]^-$ anion gives a radical-cation salt of $[\mathbf{1}][anion]_2(PhCl)_2(MeCN)$, where mixed-valence TTF units form dimers and show a strong intramolecular spin–spin exchange interaction of $2J/k_B = -30$ and $-28$ K for the $[ClO_4]^-$ and $[BF_4]^-$ salts, respectively, between the dimer and $Cr^{3+}$. Below 23 K, the salts show a weak ferromagnetism caused by the single-ion anisotropy and/or DM interaction. The existence of the mixed-valence state of the TTF-type ligand and the remarkably strong exchange interaction between the d and $\pi$ electrons indicate that the chromium acetylide–TTF-type complex is one of the promising candidates for constructing new and novel $\pi$–d interaction systems.

## ASSOCIATED CONTENT

**Supporting Information.** X-ray crystallographic data in CIF format. This material is available free of charge via the Internet at http://pubs.acs.org.

## AUTHOR INFORMATION

**Corresponding Author**

*E-mail: nishi@ims.ac.jp. Tel: +81-564-55-7350. Fax: +81-564-54-2254.

## ACKNOWLEDGMENT

This work was supported by Grant-in-Aid for Scientific Research No. 20750119 from the Ministry of Education, Culture, Sports, Science and Technology, Japan.

## REFERENCES

(1) (a) Enoki, T.; Miyazaki, A. *Chem. Rev.* **2004**, *104*, 5449–5477. (b) Shao, X.; Yamaji, Y.; Fujiwara, H.; Sugimoto, T. *J. Mater. Chem.* **2009**, *19*, 5837–5844. (c) Hiraga, H.; Miyasaka, H.; Nakata, K.; Kajiwara, T.; Takaishi, S.; Oshima, Y.; Nojiri, H.; Yamashita, M. *Inorg. Chem.* **2007**, *46*, 9661–9671. (d) Coronado, E.; Curreli, S.; Giménez-Saiz, C.; Gómez-García, C. J.; Deplano, P.; Mercuri, M. L.; Serpe, A.; Pilia, L.; Faulmann, C.; Canadell, E. *Inorg. Chem.* **2007**, *46*, 4446–4457. (e) Coronado, E.; Galan-Mascaros, J. R.; Gómez-García, C. J.; Laukhin, V. *Nature* **2000**, *408*, 447–449. (f) Nishijo, J.; Ogura, E.; Yamaura, J.; Miyazaki, A.; Enoki, T.; Takano, T.; Kuwatani, Y.; Iyoda, M. *Solid State Commun.* **2000**, *116*, 661–664. (g) Rabaça, S.; Almeida, M. *Coord. Chem. Rev.* **2010**, *254*, 1493–1508. (h) Reinheimer, E. W.; Olejniczak, I.; Łapiński, A.; Świetlik, R.; Jeannin, O.; Fourmigué, M. *Inorg. Chem.* **2010**, *49*, 9777–9787.

(2) (a) Ishikawa, M.; Asari, T.; Matsuda, M.; Tajima, H.; Hanasaki, N.; Naito, T.; Inabe, T. *J. Mater. Chem.* **2010**, *20*, 4432–4438. (b) Fujiwara, H.; Hayashi, T.; Sugimoto, T.; Nakazumi, H.; Noguchi, S.; Li, L.; Yokogawa, K.; Yasuzuka, S.; Murata, K.; Mori, T. *Inorg. Chem.* **2006**, *45*, 5712–5714. (c) Nishijo, J.; Miyazaki, A.; Enoki, T.; Watanabe, R.; Kuwatani, Y.; Iyoda, M. *Inorg. Chem.* **2005**, *44*, 2493–2506.

(3) Kobayashi, H.; Tomita, H.; Naito, T.; Kobayashi, A.; Sakai, F.; Watanabe, T.; Cassoux, P. *J. Am. Chem. Soc.* **1996**, *118*, 368–377.

(4) (a) Uji, S.; Shinagawa, H.; Terashima, T.; Yakabe, T.; Terai, Y.; Tokumoto, M.; Kobayashi, A.; Tanaka, H.; Kobayashi, H. *Nature* **2001**, *410*, 908–910. (b) Fujiwara, H.; Kobayashi, H.; Fujiwara, E.; Kobayashi, A. *J. Am. Chem. Soc.* **2002**, *124*, 6816–6817.

(5) (a) Lorcy, D.; Bellec, N.; Fourmigué, M.; Avarvari, N. *Coord. Chem. Rev.* **2009**, *253*, 1398–1438. (b) Dias, S. I. G.; Neves, A. I. S.; Rabaça, S.; Santos, I. C.; Almeida, M. *Eur. J. Inorg. Chem.* **2008**, 4728–4734. (c) Uzelmeier, C. E.; Smucker, B. W.; Reinheimer, E. W.; Shatruk, M.; O'Neal, A. W.; Fourmigué, M.; Dunbar, K. R. *Dalton Trans.* **2006**, 5259–5268. (d) Wang, L.; Zhang, B.; Zhang, J. *Inorg. Chem.* **2006**, *45*, 6860–6863. (e) Qin, Y.-R.; Zhu, Q.-Y.; Huo, L.-B.; Shi, Z.; Bian, G.-Q.; Dai, J. *Inorg. Chem.* **2010**, *49*, 7372–7381. (f) Kolotilov, S. V.; Cador, O.; Pointillart, F.; Golhen, S.; Gal, Y. L.; Gavrilenko, K. S.; Ouahab, L. *J. Mater. Chem.* **2010**, *20*, 9505–9514. (g) Pointillart, F.; Gal, Y. L.; Golhen, S.; Cador, O.; Ouahab, L. *Inorg. Chem.* **2008**, *47*, 9730–9732. (h) Miyazaki, A.; Ogyu, Y.; Justaud, F.; Ouahab, L.; Cauchy, T.; Halet, J.-F.; Lapinte, C. *Organometallics* **2010**, *29*, 4628–4638. (i) Vacher, A.; Barrière, F.; Roisnel, T.; Lorcy, D. *Chem. Commun.* **2009**, 7200–7202. (j) Setifi, F.; Ouahab, L.; Golhen, S.; Yoshida, Y.; Saito, G. *Inorg. Chem.* **2003**, *42*, 1791–1973.

(6) Náfrádi, B.; Olariu, A.; Forró, L.; Mézière, C.; Batail, P.; Jánossy, A. *Phys. Rev. B* **2010**, *81*, 224438.

(7) (a) Wautelet, P.; Moigne, J. L.; Videva, V.; Turek, P. *J. Org. Chem.* **2003**, *68*, 8025–8036. (b) Venkatesan, K.; Fox, T.; Schmalle, H. W.; Berke, H. *Organometallics* **2005**, *24*, 2834–2847.

(8) Nishijo, J.; Judai, K.; Numao, S.; Nishi, N. *Inorg. Chem.* **2009**, *48*, 9402–9408.

(9) (a) John, D. E.; Moore, A. J.; Bryce, M. R.; Batsanov, A. S.; Leech, M. A.; Howard, A. K. *J. Mater. Chem.* **2000**, *10*, 1273–1279. (b) Bakac, A.; Espenson, J. H. *Inorg. Chem.* **1992**, *31*, 1108–1110. (c) Wright-Garcia, K.; Basinger, J.; Williams, S.; Hu, C.; Wagenknecht, P. S. *Inorg. Chem.* **2003**, *42*, 4885–4890. (d) Grisenti, D. L.; Thomas, W. W.; Turlington, C. R.; Newsom, M. D.; Priedemann, C. J.; Van Derveer, D. G.; Wagenknecht, P. S. *Inorg. Chem.* **2008**, *47*, 11452–11454.

(10) Burla, M. C.; Caliandro, R.; Camalli, M.; Carrozzini, B.; Cascarano, G. L.; De Caro, L.; Giacovazzo, C.; Polidori, G.; Spagna, R. *J. Appl. Crystallogr.* **2005**, *38*, 381–388.

(11) Sheldrick, G. M. *Acta Crystallogr., Sect. A* **2008**, *64*, 112–122.

(12) Khodorkovsky, V.; Edžifna, A.; Neilands, O. *J. Mol. Electron.* **1989**, *5*, 33–36. The oxidation potentials in this reference are obtained using a SCE reference electrode. We convert the values by using the potential of the $Ag/Ag^+$ reference electrode (0.3 V vs SCE).

(13) Burla, M. C.; Caliandro, R.; Camalli, M.; Carrozzini, B.; Cascarano, G. L.; De Caro, L.; Giacovazzo, C.; Polidori, G.; Spagna, R. *J. Appl. Crystallogr.* **2005**, *38*, 381–388.

(14) Miller, J. S.; Drillon, M. *Magnetism: Molecules to Materials*; Wiley-VCH: Weinheim, Germany, 2001; Vol. I. It should be noted that the definition of exchange interaction "J" in the reference is equal to "2J" in this report.

(15) Solano-Peralta, A.; Sosa-Terres, M. E.; Flores-Alamo, M.; El-Mkami, H.; Smith, G. M.; Toscano, R. A.; Nakamura, T. *Dalton Trans.* **2004**, 2444–2449.

(16) (a) Baker, J. M.; Bleaney, B.; Bowers, K. D. *Proc. Phys. Soc. B* **1956**, *69*, 1205. (b) Pedersen, E.; Toftlund, H. *Inorg. Chem.* **1974**, *13*, 1603–1612.

(17) (a) Nagata, K.; Tazuke, Y. *J. Phys. Soc. Jpn.* **1972**, *32*, 337–345. (b) Ohta, H.; Kirita, K.; Kunimoto, T.; Okubo, S.; Hosokoshi, Y.; Katoh, K.; Inoue, K.; Ogasahara, A.; Miyashita, S. *J. Phys. Soc. Jpn.* **2002**, *71*, 2640–2643. (c) Setifi, F.; Golhen, S.; Ouahab, L.; Miyazaki, A.; Okabe, K.; Enoki, T.; Toita, T.; Yamada, J. *Inorg. Chem.* **2002**, *41*, 3786–3790. (d) Kataev, V.; Choi, K.-Y.; Grüninger, M.; Ammerahl, U.; Büchner, B.; Freimuth, A.; Revcolevschi, A. *Phys. Rev. Lett.* **2001**, *86*, 2882–2885.

(18) (a) Dzyaloshinsky, I. *J. Phys. Chem. Solids* **1958**, *4*, 241–255. (b) Moriya, T. *Phys. Rev.* **1960**, *120*, 91–98.